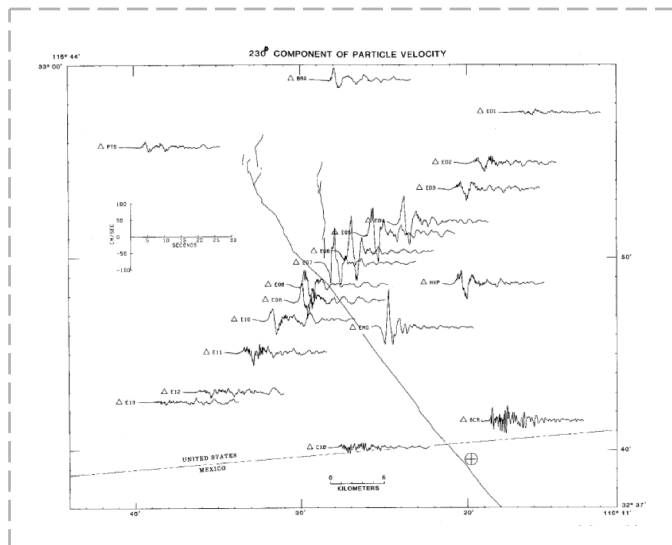


Accounting for Near-Fault Effects on GMPEs

Report produced in the context of the Global Project
“GEM Ground Motion Prediction Equations”



Jack W. Baker¹, Brian Choiu², Mustafa Erdik³, Paul Somerville⁴, Walter Silva⁵,

¹ Stanford University ² California Department of Transportation ³ Bogazici University, ⁴ URS Corporation and Macquarie University, ⁵ Pacific Earthquake Engineering and Analysis

Accounting for Near-Fault Effects on GMPEs

GEM Ground Motion Prediction Equations

Version: 1.0.0

Author(s): Jack W. Baker, Brian Chou, Mustafa Erdik, Paul Somerville, Walter Silva

Date: March 2013

Copyright © 2013 Jack W. Baker, Brian Chou, Mustafa Erdik, Paul Somerville, Walter Silva. Except where otherwise noted, this work is made available under the terms of the [Creative Commons license CC BY 3.0 Unported](https://creativecommons.org/licenses/by/3.0/)

The views and interpretations in this document are those of the individual author(s) and should not be attributed to the GEM Foundation. With them also lies the responsibility for the scientific and technical data presented. The authors do not guarantee that the information in this report is completely accurate.

Citation: Baker, J.W., B. Chou, M. Erdik, P. Somerville, W. Silva (2013) Accounting for near-fault effects on GMPEs, report produced in context of GEM GMPE project, available from <http://www.nexus.globalquakemodel.org/gem-gmpes>



ABSTRACT

Most ground-motion prediction equations (GMPEs) do not provide predictions that account explicitly for near-fault effects such as rupture directivity. A variety of models are available, however, that modify GMPE predictions to account for directivity, or to capture polarization of response spectra in the near-fault region. In addition to standard GMPE parameters such as earthquake magnitude and distance, these models typically use the earthquake hypocenter location and possibly other information about slip direction to infer whether a given site is likely to experience directivity effects, and amplifies or de-amplifies the GMPE prediction appropriately. This report presents an overview of published methods for adjusting GMPEs to include directivity effects, as well as directionality effects that are sometimes considered to be related to near-fault effects. Recommendations for the use of these models were developed by surveying all published models of this type, noting the ground motion data sets used in their calibration and the range of seismological conditions for which they are valid (e.g., active crustal earthquakes versus subduction or stable continental earthquakes). These results are intended for use by the Global Earthquake Model (GEM) project. These topics comply with the objectives of the GEM Global GMPEs project, coordinated by the Pacific Earthquake Engineering Research Center (PEER), but the findings may also be of use more generally.

Keywords: GMPE, attenuation, near-fault effects, ground motion, hazard

ACKNOWLEDGEMENTS

This study was funded by the GEM Foundation as part of the Pacific Earthquake Engineering Research Center's (PEER's) Global GMPEs project. Any opinions, findings, and conclusions or recommendations expressed in this material are those of the authors and do not necessarily reflect those of the sponsors.

TABLE OF CONTENTS

	Page
ABSTRACT	ii
ACKNOWLEDGEMENTS	iii
TABLE OF CONTENTS	iv
LIST OF FIGURES	v
LIST OF TABLES	vi
1 Introduction	2
2 Directivity Effects	5
2.1 Background	5
2.2 Models for Active Crustal Tectonic Regions.....	6
2.3 Models for Stable Continental Regions.....	8
2.4 Models for Subduction Regions	8
2.5 Use of Ground Motion Simulations to Calibrate Directivity Predictions.....	8
2.6 Recommendations for Inclusion of Directivity Effects in GMPEs.....	9
3 Directionality Effects	10
3.1 Background	10
3.2 Models for Converting between Sa_{GM} , Sa_{RotD50} , and $Sa_{GMRotI50}$	11
3.3 $Sa_{RotD100}$ Models for Active Crustal Tectonic Regions.....	12
3.4 $Sa_{RotD100}$ Models for Stable Continental Regions.....	15
3.5 $Sa_{RotD100}$ Models for Subduction Regions	16
3.6 Recommendations for Inclusion of Directionality Effects	16
4 Conclusions	19
REFERENCES	20

LIST OF FIGURES

	Page
Figure 1.1 Strike normal ground velocities from the 1992 Landers earthquake (from Somerville <i>et al</i> [1997]).	3
Figure 1.2 Illustration of orientations of motion from fling step and directivity effects in strike slip and dip-slip ruptures (figure from NIST [2012] and adapted from Somerville [2002]).	4
Figure 2.1 (a) Strike normal ground velocities, and (b) strike parallel ground velocities from the 1979 Imperial Valley earthquake (from Archuleta 1982).	6
Figure 3.1 Geometric mean ratio of $Sa_{RotD50}/Sa_{GMRotI50}$ observed from the PEER NGA West database (figure adapted from Boore 2010).	12
Figure 3.2 Published geometric mean ratios of $Sa_{RotD100}/Sa_{GMRotI50}$ in active crustal tectonic regions.	14
Figure 3.3 Geometric mean ratios of $Sa_{RotD100}/Sa_{GMRotI50}$ in stable continental regions from Huang <i>et al</i> [2012] and the NGA East project [Baker 2012], compared with the equivalent Baker and Shahi [2012] ratios for active crustal tectonic regions.	16
Figure 3.4 Plots of recommended ratios for conversion of median GMPE predictions to account for directionality effects.	18

LIST OF TABLES

	Page
Table 3.1	
Selected definitions of spectral accelerations for multi-component ground motions.....	10
Table 3.2	
Recommended ratios for conversion of median GMPE predictions to account for directionality effects.....	17

1 Introduction

This report summarizes the phenomena of near-fault and directionality effects, and provides recommendations for Task 4 of the GEM Global GMPEs-PEER project, with the objective to provide guidance on accounting for these effects in ground motion prediction equations. Specifically, two phenomena—directivity and directionality—are described and methods for accounting for these issues are discussed.

The first phenomenon of interest in this report is near-fault directivity. Ground motion prediction equations (GMPEs) provide predicted distributions of ground motion parameters as a function of explanatory variables such as earthquake magnitude, rupture distance and site conditions. One ground motion phenomenon that is not well-captured by standard explanatory variables is near-fault directivity, which occurs when a fault rupture propagates towards the site at approximately the shear wave velocity, causing most of the seismic energy to arrive as a high-amplitude, short-duration ground motion. Near-fault directivity can be included in GMPEs, however, by taking advantage of GMPE-adjustment models. These adjustment models specify modifications to the underlying GMPE, as a function of additional explanatory variables that are not included in the underlying GMPE but which are indicative of conditions under which directivity is or is not expected.

The second phenomenon of interest in this report is ground motion directionality. Ground motions produce shaking in three dimensions (they also produce rotations though those are not predicted by GMPEs). When using a GMPE to predict a ground motion parameter associated with horizontal shaking, the two-directions of shaking in the horizontal plane must be considered. The predicted ground motion parameters (e.g., spectral acceleration at a specified period, peak ground acceleration, or peak ground velocity) can be defined in a variety of ways with regard to multicomponent horizontal shaking. Common methods to quantify spectral acceleration from two-component horizontal shaking are to take the geometric mean of the spectral accelerations of the two as-recorded ground motion components, to take the maximum spectral acceleration observed when looking over all horizontal orientations, or to take the median spectral acceleration observed when looking over all horizontal orientations. A given GMPE will specify the definition of spectral acceleration being predicted, and if that definition differs from the definition desired by the hazard analyst, a model for converting between definitions is needed. Such models are discussed below. This phenomenon is grouped with “near-fault effects” in some cases, because the relationship between these various definitions depends upon the polarization of the ground motion, and some aspects of polarization may differ in the near-field relative to the far field.

Before discussing the above two phenomena in more detail, a few other near-fault effects should be mentioned briefly for completeness. In addition to influencing ground motion peak spectral amplitudes, near-fault directivity also affects ground motion duration. In forward-directivity cases, where wave arrivals are compressed in time, ground motion durations are generally decreased, while in backward-directivity cases the durations are increased relative to no-directivity conditions. This can be observed in Figure 1.1, which shows observed velocity time histories from the 1992 Landers earthquake in forward-directivity and backward-directivity conditions. Somerville *et al* [1997] proposed adjustments to ground

motion duration based on geometric parameters associated with directivity. But because prediction of ground motion duration is not a focus of this project, this issue is not discussed further.

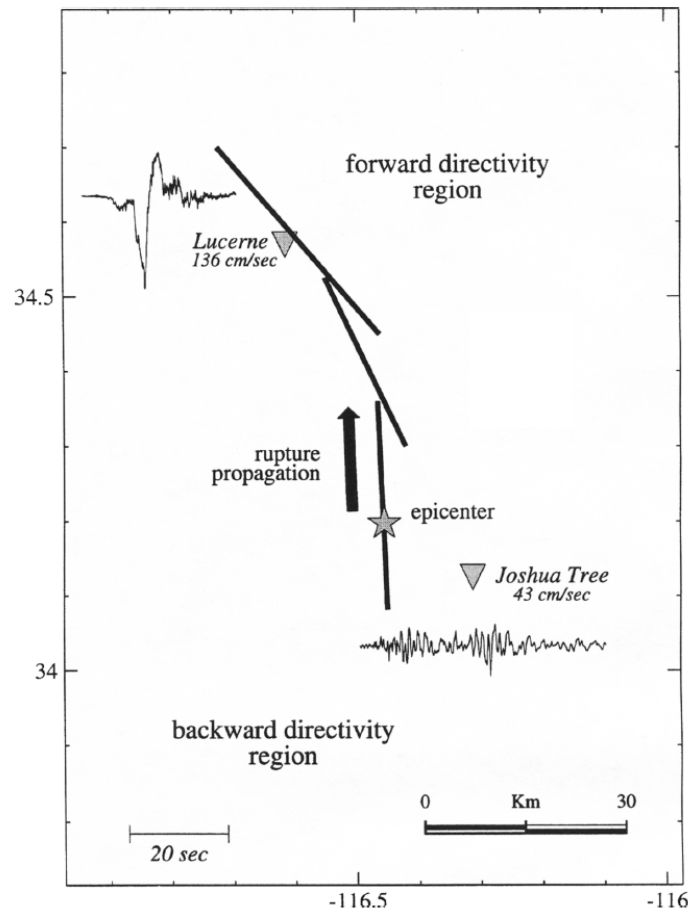


Figure 1.1 Strike normal ground velocities from the 1992 Landers earthquake (from Somerville *et al* [1997]).

In addition to directivity, another near-fault effect of potential interest is static fling. “Fling step” is permanent ground displacement caused by faulting and crustal deformation. A schematic illustration of the contributions of directivity and fling step to ground motions is shown in **Figure 1.2**. While fling step may have some effect on dynamic response of structures, there are no resources available today to include the effect in GMPs. Due to the lack of models for modifying GMPs to include fling step, this issue is not discussed further here. These crustal deformations can also result in static displacement offsets at crossings of surface-rupturing earthquakes. These deformations can be very damaging to infrastructure and other systems that cross faults. There are models available for predicting these deformations, but they are outside the scope of this project and therefore not discussed further.

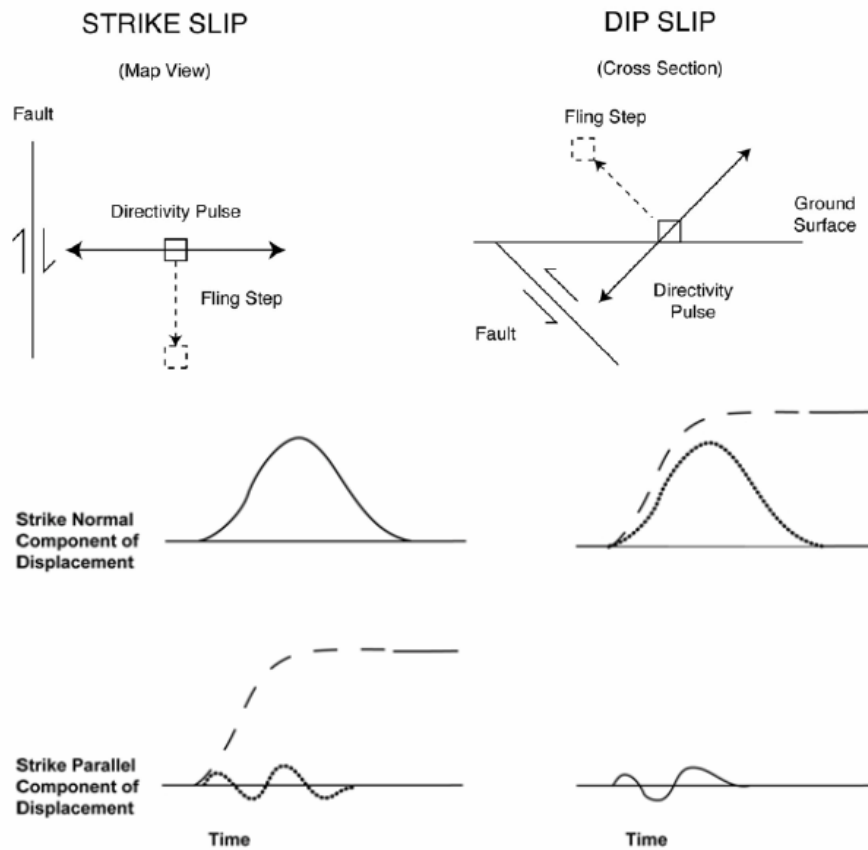


Figure D-5 Top: Schematic orientation of the rupture directivity pulse and fling step for strike-slip (left) and dip-slip (right) faulting. Bottom: Schematic partition of the rupture directivity pulse and fault displacement between strike-normal and strike-parallel components of ground displacement. Waveforms containing static ground displacement are shown as dashed lines; versions of these waveforms with the static ground displacement removed are shown as dotted lines (Somerville, 2002).

Figure 1.2 Illustration of orientations of motion from fling step and directivity effects in strike slip and dip-slip ruptures (figure from NIST [2012] and adapted from Somerville [2002]).

2 Directivity Effects

2.1 Background

Directivity causes variations in ground motion spectral accelerations that are not accounted for fully by standard ground motion prediction equations. Directivity effects generally increase spectral accelerations at locations where the rupture has propagated towards the site of interest, for periods longer than approximately 0.5 seconds. At locations where the rupture has propagated away from the site, spectral accelerations are generally decreased. Also associated with the “forward-directivity” high amplitude conditions is the presence of a short-duration velocity pulse. Examples of ground motions exhibiting effects of forward and backward directivity were shown earlier in **Figure 1.1** as well as in **Figure 2.1** below. As can be noted by comparing **Figure 2.1a** and b, the ground motion amplitudes in the strike-normal direction tend to be larger than in the strike-parallel direction, but there are also cases where the largest amplitudes occur in other directions [Howard *et al*, 2005]. Because the directivity effect depends upon rupture direction, additional predictor parameters not included in most GMPEs are needed to account for this effect. Most directivity models utilize some description of the amount of the rupture that has ruptured towards the site of interest in order to predict this effect. The following sub-sections will discuss specific models for predicting directivity effects. As the reference GMPE will vary with the type of seismic region being considered, directivity-modification models are also grouped according to tectonic region.

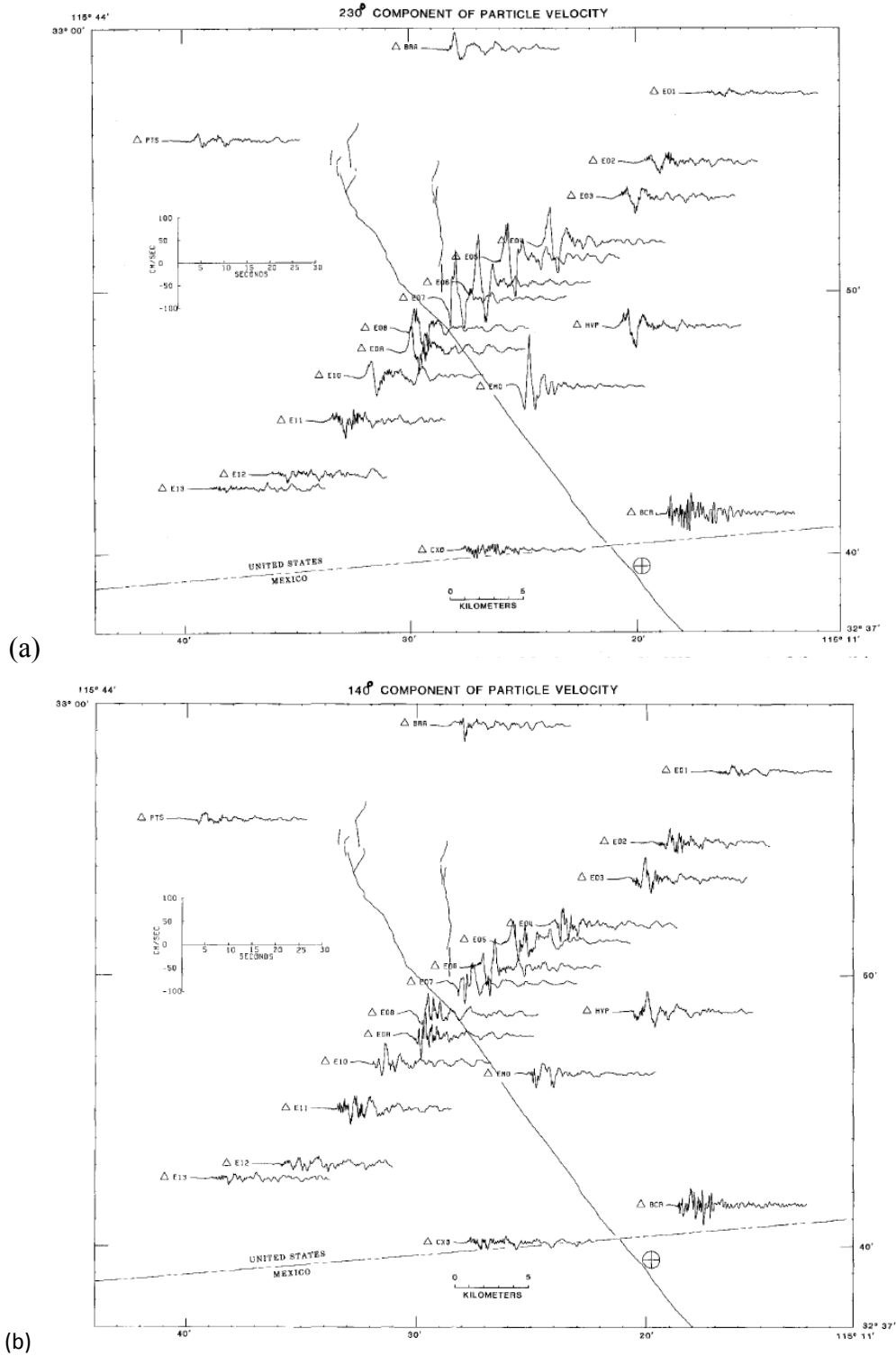


Figure 2.1 (a) Strike normal ground velocities, and (b) strike parallel ground velocities from the 1979 Imperial Valley earthquake (from Archuleta [1982]).

2.2 Models for Active Crustal Tectonic Regions

Several models have been published that modify an active crustal region GMPE to account for directivity effects (Somerville *et al* [1997]; Abrahamson [2000]; Rowshandel [2006]; Spudich *et al* [2004]; Spudich

and Chiou [2008]; Rowshandel [2010]; Shahi and Baker [2011]). These models share several features. They all provide ratios by which to multiply a base GMPE's predicted median and log standard deviation, as a function of parameters related to the geometry of the fault rupture. They all were developed with respect to active crustal region (ACR) earthquake datasets and GMPEs. They all require specification of a finite fault and a hypocenter location in addition to the standard predictive parameters used by base GMPEs, and some require additional information such as slip direction (i.e., point-source descriptions of earthquakes or source descriptions that do not specify a hypocenter are not suitable for directivity predictions). Most models also provide predictions that vary with rupture mechanism. The degree of modification provided by these models is largest at very close distances from the rupture, and at distances of greater than approximately 30 km from the fault there is often little predicted modification. One distinction among of the above models is that some are "broadband" in that the modification of the GMPE's predicted response spectrum with period is fixed in shape, while others are "narrowband" in that the spectral amplification at a given period is functionally dependent on earthquake magnitude and possibly other parameters [Somerville, 2003]. Among existing models, the Somerville *et al* [1997] model and closely related Abrahamson [2000] model are currently the most popular for site-specific hazard calculations.

The above models all utilize knowledge of a hypocenter location and rupture extent (and possibly additional information) in order to make predictions of the effect of directivity. This creates challenges for implementation in regional or global probabilistic seismic risk analysis, because it requires a seismic source model that includes randomly occurring hypocenter locations, and requires increased complexity and computation time in the prediction of ground motions [Abrahamson, 2000]. To overcome this challenge, a concept has been proposed for development of future models that avoid using a hypocenter-dependent ground motion prediction, and instead modify a non-directivity GMPE (e.g., by inflating the prediction standard deviation in the near field) to account for potential higher amplitude Sa 's that might occur due to the possible occurrence of directivity effects [Dr. Norman Abrahamson personal communication, 2011]. This "average directivity" modification could be calibrated by fixing a rupture extent, randomly locating hypocenters (e.g., Mai, Spudich and Boatwright [2005]), computing Sa distributions for each case, and computing the distribution of Sa values implied by the aggregate set of predictions. The resulting model adjustment would be magnitude and distance dependent, and possibly dependent on the location of the site of interest along fault. Predictions using this approach would differ from predictions using a non-directivity GMPE in that the non-directivity GMPEs' near-fault predictions are calibrated to predict ground motions representative of the conditions well-represented in the reference ground motion library, rather than "average directivity" conditions.

As a point of reference regarding current state-of-the art in ground motion prediction when random hypocenters are not included in the source model, the US Geological Survey (which calculates hazard without randomized hypocenters) currently makes no modifications to GMPEs to account for near-fault effects¹ (Dr. Nicolas Luco personal communication, [2011]).

¹ Note that the USGS does include modified GMPEs to represent epistemic uncertainty, and the modifications are magnitude/distance dependent, with generally larger uncertainty at close distances. While the degree of uncertainty relates to the number of ground motions available to constrain the GMPEs in each magnitude/distance range, it may also help address additional uncertainty due to directivity (i.e., the epistemic uncertainty is large for conditions where directivity might be expected).

The in-development NGA West 2 models (<http://peer.berkeley.edu/ngawest2/>) for crustal earthquakes will include predictions that utilize directivity-related geometry and supersede the above modification models, as well as an “average directivity” prediction that can be used instead if the directivity-related geometry is not available [Spudich *et al*, 2012]. These soon-to-be-available models will be the first documented cases of this approach being implemented.

2.3 Models for Stable Continental Regions

There are no known models for predicting the effects of directivity in stable continental regions (SCRs). While directivity effects should exist in SCR earthquakes, calibration of an appropriate model is not feasible in the near future, for several reasons. The most straightforward problem is that the very limited number of observations of near-field ground motions from SCR earthquakes prevents calibration of a predictive model from data. Second, while one might consider adopting a directivity model for active crustal regions for use in an SCR, there are unresolved issues associated with this concept. For example, higher stress drops in stable continental regions may affect magnitude-area relationships and thus indirectly affect resulting directivity (which is dependent on magnitude and rupture dimensions) in unforeseen ways.

As a point of reference regarding state-of-the art in these regions, the US Nuclear Regulatory Commission does not have provisions for accounting for directivity effects in site-specific hazard analyses in stable continental regions [Dr. Annie Kammerer personal communication, 2011]. We found no examples worldwide of cases where directivity effects have been considered when assessing seismic hazard in a stable continental region.

2.4 Models for Subduction Regions

There are no known predictive models for directivity in either intraslab or interface subduction earthquakes. Note that from subduction earthquake rupture geometry, no onshore directivity would be expected from subduction events. There may be directivity parallel to strike due to compression in time of propagating waves, and this could possibly result in larger spectral amplitudes at onshore locations, but these events would not be expected to produce velocity pulses of the type discussed in Section 1 above. We found no examples worldwide of cases where directivity effects have been considered when assessing seismic hazard in a subduction region.

2.5 Use of Ground Motion Simulations to Calibrate Directivity Predictions

One other potential source of guidance for modifying GMPEs to include directivity effects is numerical ground motion simulations. Simulations are ideal in their ability to produce near-field ground motion data needed to study directivity, and to study variation in response spectra as earthquake rupture geometry is varied systematically. On the other hand, simulation models require accurate representation of the earthquake source if predicted directivity effects are to be consistent with empirical observations. A variety of researchers have performed ground motion simulations and reported features in the resulting ground motions related to directivity. For example, Si and Midorikawa [2004] and Hikita [2006] report observations of directivity effects from numerical simulations of active crustal earthquakes. Kato *et al* [2002] report observing directivity in numerical simulations of subduction events when the rupture propagates in the up-dip direction, but not when it propagates along strike.

Sesetyan [2007] studied the spatial variation of directivity effects from simulated time histories. Kinematic simulations have been carried out to simulate long period waves ($T \geq 2$ sec) for both hypothetical and real earthquake ruptures and the spatial variation of fault-normal to average spectral acceleration ratios were investigated. Simulation results for the strike-slip events show that the ratios of fault normal to the geometric mean of the horizontal component ($R_{FN/Mean}$) follow the same pattern regardless of the earthquake magnitude and slip distribution. This pattern is characterized by a narrow zone of $R_{FN/Mean} = 2$ around the fault which widens beyond the fault extremities. A zone of $R_{FN/Mean} = 0.5$ was observed in a region perpendicular to the fault and passing through the hypocenter. This behavior was empirically evidenced in the 2004 Parkfield earthquake recordings of the Gold Hill array. An almost V-shaped region of $R_{FN/Mean}$ contours of 1 and 1.5 intersecting at the epicenter exists in all simulations. The observed pattern is similar for all the period range (2 sec to 5 sec) where the spectral accelerations were computed.

Collins *et al* [2006] studied ground motions from three simulation procedures, and looked at response spectra residuals relative to GMPEs to search for evidence of directivity effects of the form predicted by the Somerville *et al* [1997] model. While some directivity effects were present, the results were inconsistent between the three models. The results from the Collins *et al* [2006] study were interpreted as promising with regard to the future potential of numerical simulations to guide calibration of ground motion prediction equations for effects such as directivity and magnitude scaling, no such calibration was done using these data.

While these and other similar documents indicate the future role of simulations in studying and predicting directivity effects, to date no predictive models for the impact of directivity on response spectra have been produced on the basis of ground motion simulations, and thus this field of research has not yet provided results of use to the GEM project.

2.6 Recommendations for Inclusion of Directivity Effects in GMPEs

Based on the above discussion, we provide the following recommendations for potential inclusion of directivity effects in GMPEs.

For active regions with shallow crustal seismicity, use the forthcoming NGA West 2 models. It is anticipated that these models will be able to make directivity predictions both for cases with and without a specified hypocenter. As with the use of GMPEs in general, it is recommended that multiple directivity models be used to account for epistemic uncertainty.

For other regions, there are no available models that predict directivity effects and so no modification of base GMPEs should be performed. We note that this recommendation is due to a lack of available models rather than due to a proven lack of directivity effects in such regions. In the future, if directivity models for these regions become available they could be used, though we are aware of no such models in development at present.

3 Directionality Effects

3.1 Background

Ground motions vary in intensity as a function of the orientation of interest, so there are a variety of ways to quantify intensity for multi-component ground motions. Many ground motion prediction equations predict the geometric mean of the response spectra of two horizontal components of ground motion. In some cases it may be of greater interest to know the maximum spectral value, over all possible directions, of spectral acceleration at a given periods. In addition, there are a variety of other definitions of ground motion parameters from multicomponent ground motions. For the purposes of vulnerability predictions, it is important that the ground motion intensity measure be consistent between the ground motion prediction and the vulnerability calculation, so some adjustment of ground motion predictions may be needed in some cases.

A review of most common definitions, including models for converting between definitions, is provided by Beyer and Bommer [2006]. The ground motion parameter definitions likely to be of interest to GEM (because they are predicted by recommended GMPEs or because they may be of use for inputs to fragility functions) are summarized in Table 3.1. The table uses notation for spectral accelerations, but the definitions can also be applied to PGA or PGV values.

Table 3.1 Selected definitions of spectral accelerations for multi-component ground motions

Notation	Description
Sa_{GM}	Geometric mean of spectral accelerations of the two as-recorded horizontal components
Sa_{RotD50}	Median (i.e., 50 th percentile) value of spectral accelerations computed over all rotation angles for a given ground motion
$Sa_{RotD100}$	Maximum direction (i.e., 100 th percentile) value of spectral accelerations computed over all rotation angles for a given ground motion
$Sa_{GMRotD50}$	Median value of geometric mean spectral accelerations computed over all rotation angles for a given ground motion
$Sa_{GMRotI50}$	Geometric mean spectral acceleration, computed at an orientation which minimizes the sum of differences between $Sa_{GMRotD50}$ and $Sa_{GMRotI50}$ over the usable range of oscillator periods

Note that for a given ground motion, the orientation associated at $Sa_{RotD50}(T_1)$ with in general differ from the orientation associated with $Sa_{RotD50}(T_2)$, where T_1 and T_2 are non-equal periods. The same is true for orientations of $Sa_{RotD100}$ values. The desire to find a single principle orientation for a given ground motion led to the development of the $Sa_{GMRotI50}$ definition, although identifying the single orientation results in added complexity in that definition [Boore *et al*, 2006].

Most published GMPEs are for Sa_{GM} (most models prior to 2006, and many after 2006), $Sa_{GMRotI50}$ (the 2008 NGA West models and some others after 2006) or $Sa_{GMRotD50}$ (the NGA East and NGA West 2 models, and some other models in current development). When converting GMPEs to predict Sa 's with the

various definitions in Table 3.1, one needs a ratio by which to modify median Sa predictions, as well as a ratio by which to modify the predicted log standard deviation. Those ratios in general vary by period and seismological region, as discussed below.

Before proceeding to consider modifications of Sa definition, it is important to emphasize that the Sa definition used in the GMPE and hazard component must be consistent with the Sa definition used by the fragility functions to predict damage. That is, GEM should not modify GMPEs to produce a maximum direction Sa prediction unless the structural fragility functions use a maximum direction Sa as input (see, e.g., Baker and Cornell 2006, Beyer and Bommer 2006 for further discussion).

3.2 Models for Converting between Sa_{GM} , Sa_{RotD50} , and $Sa_{GMRotI50}$

$Sa_{GMRotI50}$ [Boore *et al*, 2006] and Sa_{RotD50} [Boore, 2010] were proposed as refinements to the traditional Sa_{GM} parameter, which remove the dependence of a ground motion's Sa on the orientation of the recording instrument. All three parameters will be similar for a given ground motion, and in a probabilistic sense they will have similar means and standard deviations for ground motions resulting from a given earthquake and site condition. Beyer and Bommer [2006] found that $Sa_{GMRotI50}$ has the same mean value as Sa_{GM} , and that the ratio between the two had a very small log standard deviation (0.03 to 0.04), indicating that their values are nearly identical for recorded ground motions. Boore [2010] found that the geometric mean ratio of $Sa_{RotD50}/Sa_{GMRotI50}$ of recorded ground motions was slightly larger than 1, as shown in Figure 3.1. Boore [2010] also reports that standard deviations of $Sa_{RotD50}/Sa_{GMRotI50}$ ratios vary from 1.05 to 1.07, depending upon period. But that standard deviation includes uncertainty in both Sa_{RotD50} and $Sa_{GMRotI50}$, so it is not simply additive to the log standard deviation for a predictive model for $Sa_{GMRotI50}$; the log standard deviation for a Sa_{RotD50} GMPE would be larger than the log standard deviation for a $Sa_{GMRotI50}$ GMPE by less than 4% [Boore, 2010].

All of the studies cited in this section were calibrated using ground motions from shallow crustal earthquakes in active seismic regions. To date no similar models have been produced using ground motions from other regions.

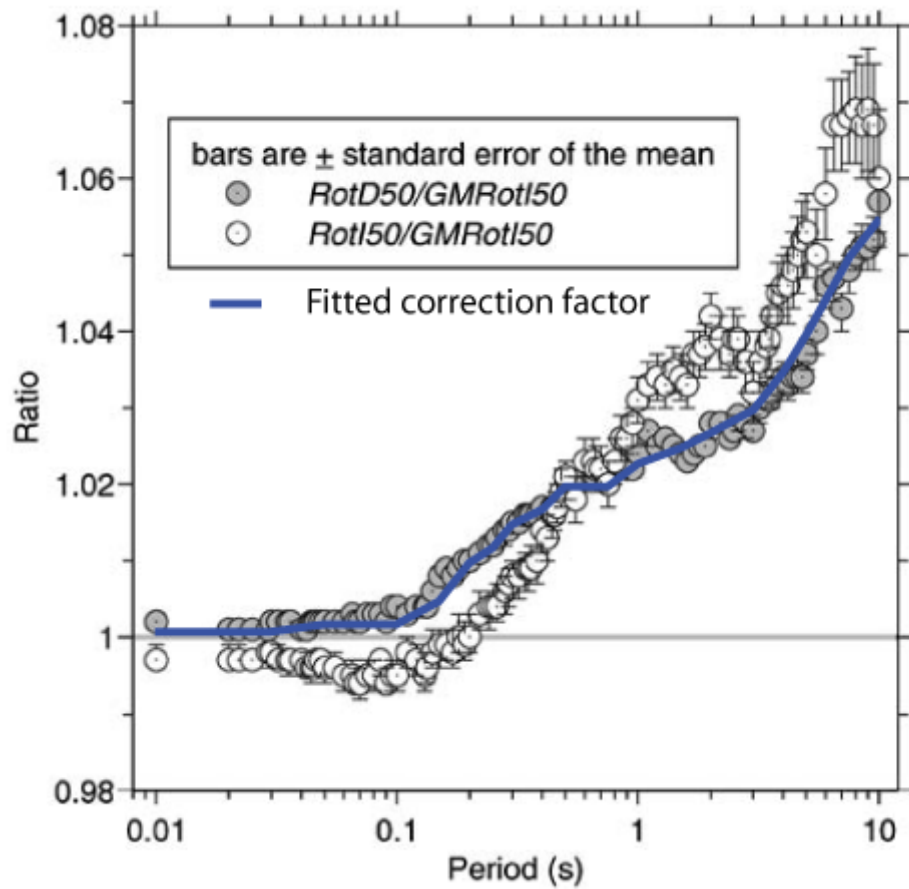


Figure 3.1 Geometric mean ratio of $Sa_{RotD50}/Sa_{GMRotI50}$ observed from the PEER NGA West database (figure adapted from Boore 2010).

3.3 $Sa_{RotD100}$ Models for Active Crustal Tectonic Regions

A variety of researchers have studied ratios between $Sa_{RotD100}$ and $Sa_{GMRotI50}$ values in observed ground motions from earthquakes in active crustal tectonic regions (Beyer and Bommer [2006]; Campbell and Bozorgnia [200]; Watson-Lamprey and Boore [200]; Huang *et al* [2008, 2012]). Additionally, the NGA West 2 project is currently performing the same calculations from a newly-expanded database of recorded strong ground motions [Shahi and Baker, 2012]. Figure 3.2 shows predictions of geometric mean $Sa_{RotD100}/Sa_{GMRotI50}$ ratios from the above-cited sources².

² The NGA West 2 project data does not include $Sa_{GMRotI50}$ values, so the ratios in The models in **Figure 3.2** generally find that median $Sa_{GMRotI50}$ predictions should be multiplied by approximately 1.2 at short periods ($T < 0.1$ sec) and approximately 1.3 at longer periods ($T > 1$ sec). None of the authors found strong trends in these ratios with magnitude, distance or directivity indicators. Watson-Lamprey and Boore [2007] noted slight distance, magnitude and radiation pattern dependence, but stated that “for most engineering applications the conversion factors independent of those variables can be used.” Similarly, Shahi and Baker’s [2012] analysis of the NGA West 2 data set indicates a slight trend with distance (with distances of < 3 km having ratios approximately 0.02 larger than the average ratios for the entire library of ground motions). Similarly, the differences between the

All five sets of ratios in Figure 3.2 are very similar. This is in part because the data sets used in each case were similar, and in part because these ratios appear to be very stable in general, as will be discussed further below. First, a brief summary of the data sets used for calibration is provided. The Beyer and Bommer [2006] ratios were developed from 949 ground motions in the PEER NGA database, with magnitudes ranging from 4.2 to 7.9 and distances ranging from 5km to 200 km. The Beyer and Bommer ratios plotted in **Figure 3.2** are from a fitted function rather than raw data, and this is the likely source of the slight discrepancy between those ratios and the others at some periods. Campbell and Bozorgnia [2007] used 1561 ground motions from the PEER NGA database over their range of usable periods. The Watson-Lamprey and Boore [2007]) ratios used the entire PEER NGA database with two-component recordings—a total of 3529 ground motions—but only considered spectra for periods less than the maximum usable period as documented in that publication. Huang *et al* [2012] computed median ratios from 91 ground motions in the PEER NGA database selected to have magnitudes of greater than 6.5, distances of less than 15km, and to exclude recordings from the Chi-Chi, Taiwan, earthquake. The Shahi and Baker [2012] data shown in **Figure 3.2** use the expanded NGA West 2 database with approximately 3000 ground motions, and use a mixed-effects model to estimate median ratios in a manner that prevents well-recorded earthquakes from disproportionately influencing the results.

four models in **Figure 3.2** are often less than 0.02 and the results can similarly be interpreted as essentially identical.

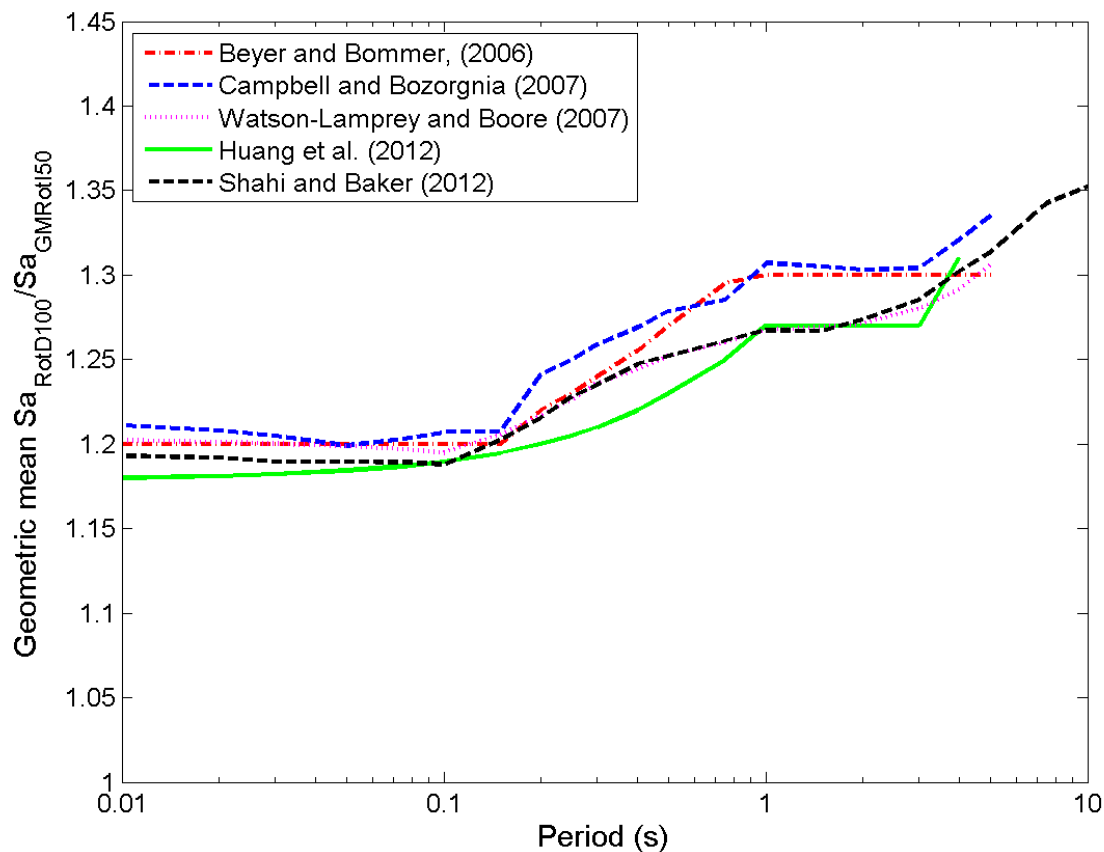


Figure 3.2 were obtained by computing geometric mean $Sa_{RotD100}/Sa_{RotD50}$ ratios, and then multiplying those by the geometric mean $Sa_{RotD50}/Sa_{GMRotI50}$ ratios from Boore (2010).

The models in **Figure 3.2** generally find that median $Sa_{GMRot150}$ predictions should be multiplied by approximately 1.2 at short periods ($T < 0.1$ sec) and approximately 1.3 at longer periods ($T > 1$ sec). None of the authors found strong trends in these ratios with magnitude, distance or directivity indicators. Watson-Lamprey and Boore [2007] noted slight distance, magnitude and radiation pattern dependence, but stated that “for most engineering applications the conversion factors independent of those variables can be used.” Similarly, Shahi and Baker’s [2012] analysis of the NGA West 2 data set indicates a slight trend with distance (with distances of < 3 km having ratios approximately 0.02 larger than the average ratios for the entire library of ground motions). Similarly, the differences between the four models in **Figure 3.2** are often less than 0.02 and the results can similarly be interpreted as essentially identical.

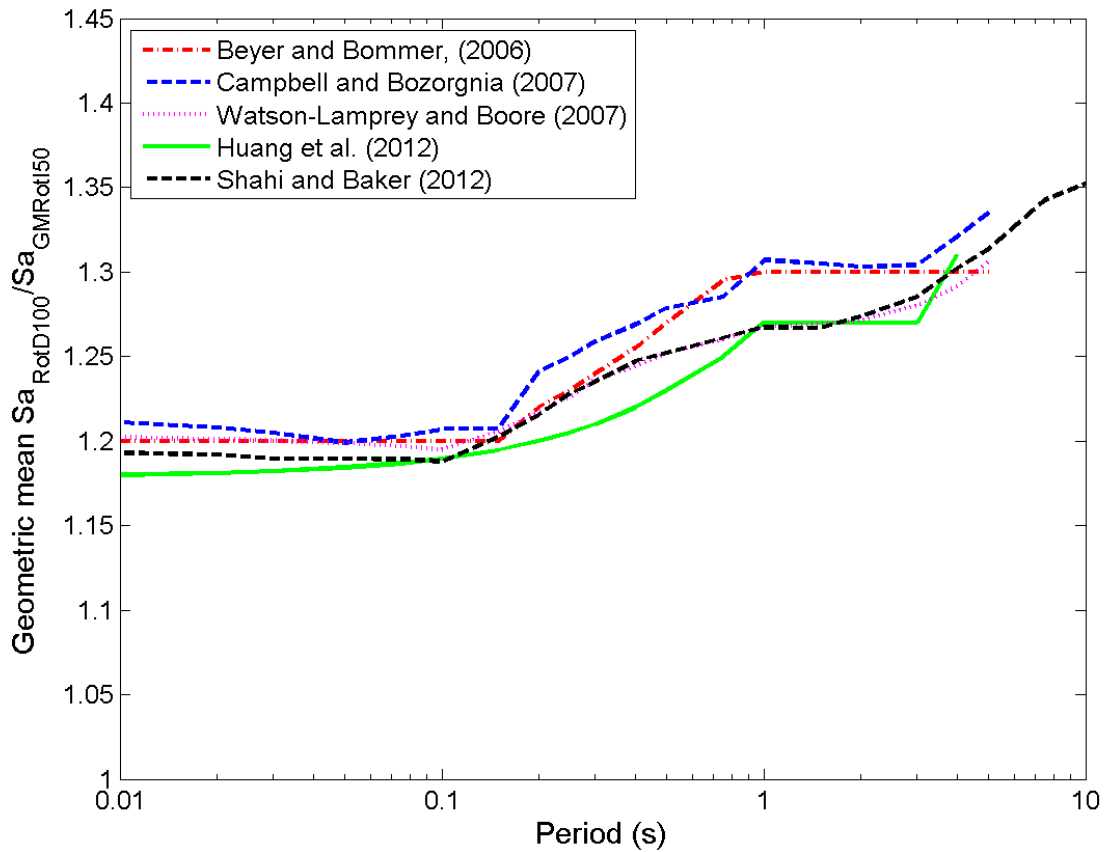


Figure 3.2 Published geometric mean ratios of $Sa_{RotD100}/Sa_{GMRot150}$ in active crustal tectonic regions.

The standard deviation for $Sa_{RotD100}$ predictions is slightly larger than the standard deviation for $Sa_{GMRot150}$ predictions (Beyer and Bommer [2006]; Watson-Lamprey and Boore [2007]). For example, Watson-Lamprey and Boore [2007] report that the Boore and Atkinson (2008) GMPE log standard deviation of 0.645 for $Sa_{GMRot150}$ (1 sec) would be increased to 0.666 for $Sa_{RotD100}$ (1 sec)—an increase of 3%, and a variation that is less than the typical variation of standard deviations between GMPEs predicting the same ground motion parameter. For this reason, the standard deviation of $Sa_{RotD100}$ might be reasonably approximated as equal to the standard deviation of $Sa_{GMRot150}$. This approximation has practical advantages, because if only the geometric mean of Sa is affected by the change of definition, it is possible to convert between definitions even after a hazard analysis has been performed for one definition. For example, the USGS multiplies spectral acceleration values with a given return period by the constants specified in NEHRP [2009] in order to make $Sa_{RotD100}$ maps from $Sa_{GMRot150}$ maps, rather than re-computing the maps with new GMPMs for $Sa_{RotD100}$ that have been modified to include both median and standard deviation adjustments. If a more refined estimate of the standard deviation of $Sa_{RotD100}$ is desired, Beyer

and Bommer [2006], Campbell and Bozorgnia [2007] and Watson-Lamprey and Boore [2007]) provide models for this adjustment.

3.4 $Sa_{RotD100}$ Models for Stable Continental Regions

The only currently available $Sa_{RotD100}/Sa_{GMrot150}$ ratios from stable continental region (SCR) ground motions exist in the grey literature (Huang *et al* [2012]; Baker [2012]). The Huang *et al* [2012] ratios were computed from 63 Central and Eastern North American ground motions with magnitudes of 4 or greater. Baker [2012] computed geometric mean ratios of $Sa_{RotD100}/Sa_{RotD50}$ from a database of 5896 stable continental region ground motions ranging in magnitude from 2 to 7 and in epicentral distance from 1 to 3000 km. Baker observed no strong trends in $Sa_{RotD100}/Sa_{GMrot150}$ ratios with magnitude or distance, so the entire dataset was used to compute these ratios, though due to restrictions on the usable period range, at some periods only a small fraction of the motions could be used for the analysis. The $Sa_{RotD100}/Sa_{RotD50}$ ratios are multiplied by the geometric mean $Sa_{RotD50}/Sa_{GMrot150}$ ratios from Boore [2010] to obtain $Sa_{RotD100}/Sa_{GMrot150}$ ratios that can be compared to the Huang *et al* [2012] results. The ratios from Huang *et al* [2012] and Baker [2012] are shown in **Figure 3.3**, along with corresponding active crustal region ratios from Baker and Shahi [2012]) for comparison. It is notable that the Baker [2012] ratios are very similar to the active crustal region ratios, while the Huang *et al* ratios are significantly higher. The Huang *et al* study used a small data set, so the results were perhaps influenced by that limited data. Further, $Sa_{RotD100}/Sa_{GMrot150}$ ratios should be influenced primarily by polarization of the ground motion, and there isn't a physical reason to expect significantly different polarization in SCR ground motions relative to motions from active seismic region crustal earthquakes. For these reasons, we believe the Baker [2012] ratios from the NGA East data to be the most reliable representation of $Sa_{RotD100}/Sa_{GMrot150}$ ratios for Stable Continental Regions.

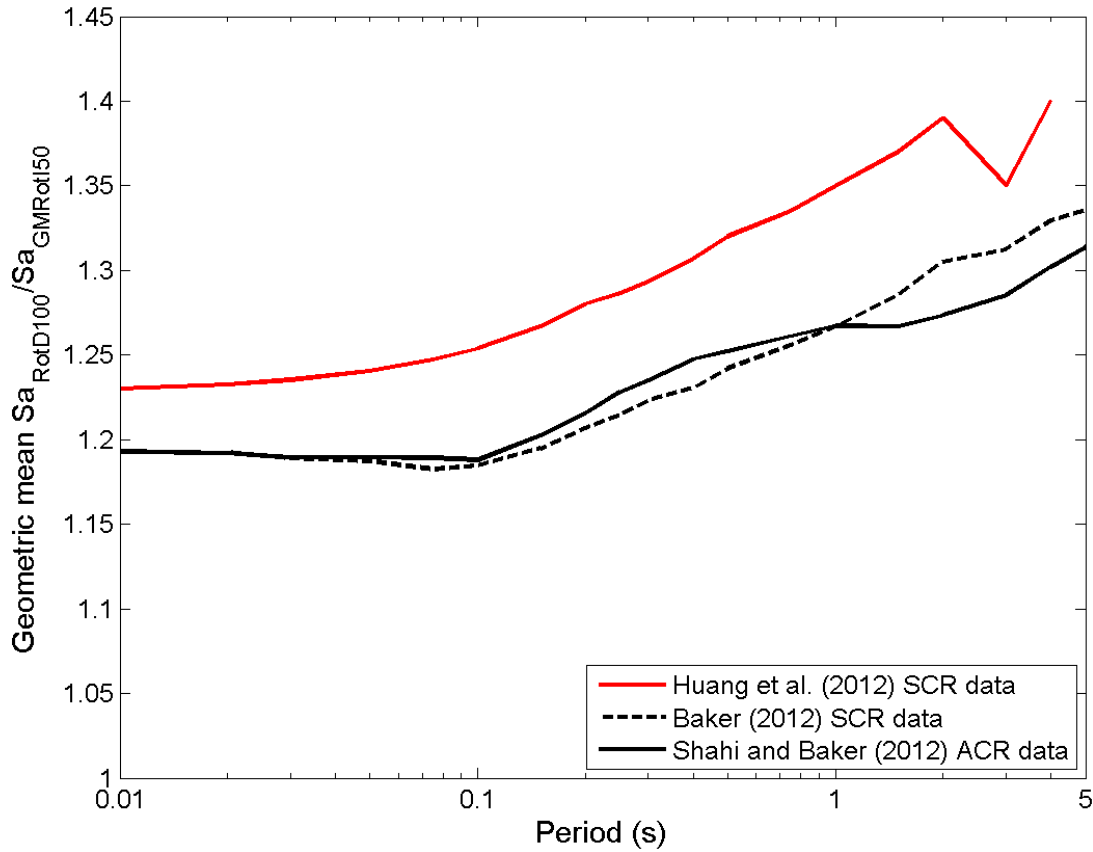


Figure 3.3 Geometric mean ratios of $Sa_{RotD100}/Sa_{GMRotI50}$ in stable continental regions from Huang *et al* [2012] and the NGA East project [Baker 2012], compared with the equivalent Baker and Shahi [2012] ratios for active crustal tectonic regions.

3.5 $Sa_{RotD100}$ Models for Subduction Regions

There are currently no published models for, or studies of, $Sa_{RotD100}/Sa_{RotD50}$ ratios in subduction earthquake ground motions. The NGA Subduction project [Bozorgnia, 2012] will address this topic, so it is anticipated that a model for these ratios will be available in the near future.

Random vibration principles suggest that $Sa_{RotD100}/Sa_{RotD50}$ ratios are likely to be comparable to ratios from other ground motions, or perhaps smaller, as the longer duration shaking of large-magnitude subduction events should lead to less polarization of the resulting ground motion response spectra. Preliminary unpublished work from the NGA Subduction project suggests that this is the case, though more careful study is needed to provide quantitative results.

In the absence of available models calibrated from subduction ground motions, it is recommended that $Sa_{RotD100}/Sa_{RotD50}$ ratios from active crustal region ground motions should be used at present as an approximate representation of directionality effects in subduction regions.

3.6 Recommendations for Inclusion of Directionality Effects

Based on the above discussion, we provide the following recommendations for potential inclusion of directionality effects in GMPEs.

To convert an Sa_{RotD50} GMPE to predict $Sa_{RotD100}$, multiply the median predictions by the ratios developed by Shahi and Baker [2012]. To convert an Sa_{GM} or $Sa_{GMRot150}$ GMPE to predict Sa_{RotD50} , use the ratios developed by Boore [2010]. These ratios are summarized in Table 3.2 and plotted in Figure 3.4. Both of these sets of ratios were calibrated using active crustal region ground motions, but could be applied globally if needed (due to the lack of comparable models calibrated for other tectonic regions, and because the limited available data from other regions suggests that these ratios are rather stable globally).

Table 3.2 Recommended ratios for conversion of median GMPE predictions to account for directionality effects.

Period (s)	$Sa_{RotD100}/Sa_{RotD50}$, (from Baker and Shahi, [2012])	$Sa_{RotD50}/Sa_{GMRot150}$ (from Boore [2010])
0.02	1.19	1.00
0.05	1.19	1.00
0.1	1.19	1.00
0.2	1.20	1.01
0.3	1.22	1.02
0.5	1.23	1.02
1	1.24	1.02
2	1.24	1.03
3	1.25	1.03
4	1.26	1.04
5	1.26	1.04
7.5	1.28	1.05
10	1.28	1.06
PGA	1.19	1.00
PGV	1.22	

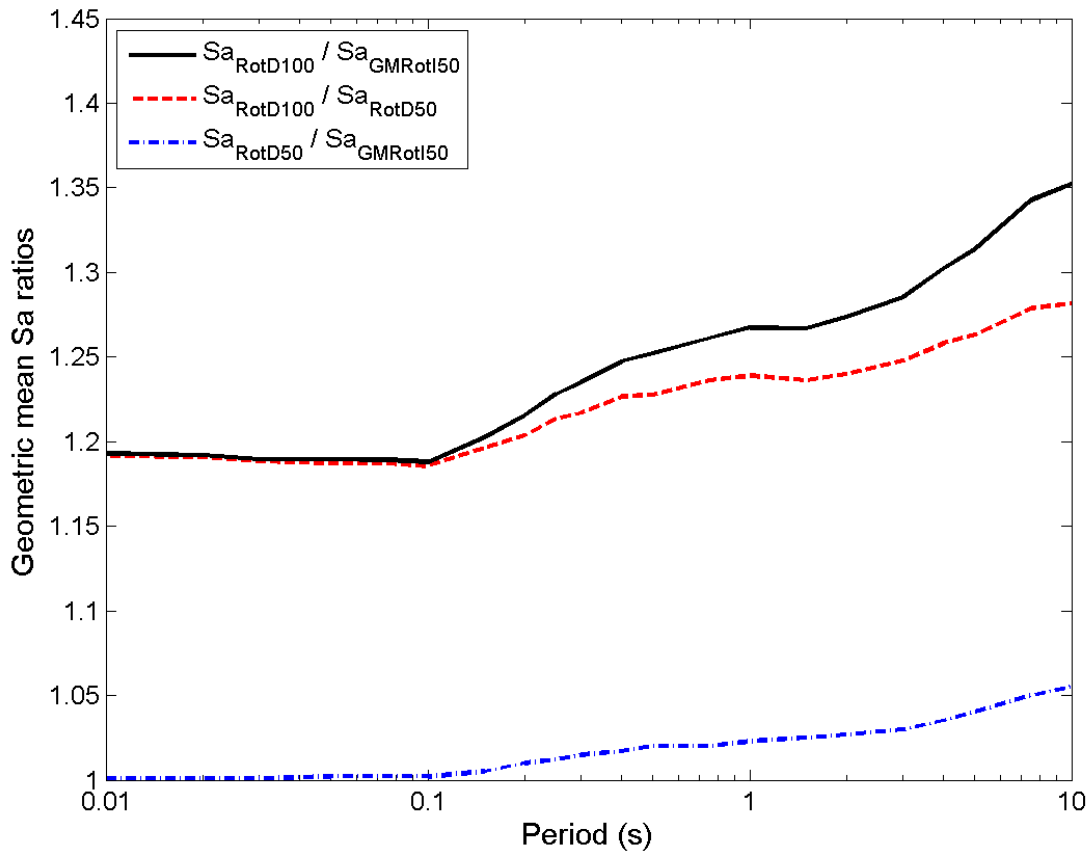


Figure 3.4 Plots of recommended ratios for conversion of median GMPE predictions to account for directionality effects.

There is relatively small variability in $Sa_{RotD100}/Sa_{RotD50}$ and $Sa_{RotD50}/Sa_{GMRotI50}$ ratios relative to the scatter in the base Sa observations, so a reasonable approximation is to use the standard deviation of underlying GMPE can as the standard deviation of the $Sa_{RotD100}$ prediction obtained using the ratios of Table 3.2. This approximation is correct to within a few percent, though in the case that a more precise standard deviation is desired, Watson-Lamprey and Boore [2007] provide a model for standard deviation adjustment.

We repeat the caution from above that the Sa definition used in the GMPE must be consistent with the Sa definition used by the fragility functions to predict damage. That is, these conversions should only be used to obtain an $Sa_{RotD100}$ prediction in cases where the corresponding fragility function requires $Sa_{RotD100}$ as an input.

An additional caution regarding the use of $Sa_{RotD100}$ predictions is that the spatial correlations of $Sa_{RotD100}$ values at multiple periods or multiple locations may differ from those for Sa_{RotD50} values. Correlations of $Sa_{RotD100}$ values have not yet been studied, though such studies may be warranted if $Sa_{RotD100}$ predictions become an important part of the GEM framework.

4 Conclusions

Recommendations are provided for the possible inclusion of directivity and directionality effects in GMPEs for the GEM model. At present, inclusion of these effects would be done via a modification to a base GMPE. All available published models of this type have been surveyed. There are relatively few published models of this type at present, so reference to in-development models has also been provided in cases where the project team deemed it appropriate.

Due to the relative infancy of these models relative to base GMPEs, pragmatic recommendations have been provided here to facilitate short-term implementation by GEM. It is anticipated that several research projects underway at the present will provide significant improvements to our understanding of these effects and the extent to which they vary across tectonic regions. Therefore, these pragmatic recommendations are likely to be superseded in the near future.

REFERENCES

- Abrahamson N.A. [2000] "Effects of rupture directivity on probabilistic seismic hazard analysis," *Proceedings of Sixth International Conference on Seismic Zonation*, Earthquake Engineering Research Inst., Oakland, CA.
- Archuleta R.J. [1982] "Analysis of near-source static and dynamic measurements from the 1979 Imperial Valley earthquake," *Bulletin of the Seismological Society of America*, Vol. 72, No. 6A, pp.1927–1956.
- Baker J.W. [2012] Ratios of SaRotD100 / SaRotD50 in NGA East data, Working report.
- Baker J.W., Cornell C.A. [2006] "Which spectral acceleration are you using?" *Earthquake Spectra*, Vol. 22, No. 2, pp. 293–312.
- Beyer K., Bommer J. J. [2006] "Relationships between median values and between aleatory variabilities for different definitions of the horizontal component of motion," *Bulletin of the Seismological Society of America*, Vol. 96, No. 4A, pp. 1512–1522.
- Boore D.M. [2010] "Orientation-independent, nongeometric-mean measures of seismic intensity from two horizontal components of motion," *Bulletin of the Seismological Society of America*, Vol. 100., No. 4, pp. 1830–1835.
- Boore D.M., Atkinson G.M. [2008] "Ground-motion prediction equations for the average horizontal component of PGA, PGV, and 5%-Damped PSA at spectral periods between 0.01 s and 10.0 s," *Earthquake Spectra*, Vol. 24, No. 1, pp. 99–138.
- Boore D.M., Watson-Lamprey J., Abrahamson N.A. [2006] "Orientation-independent measures of ground motion," *Bulletin of the Seismological Society of America*, Vol. 96, No. 4A, pp. 1502–1511.
- Bozorgnia Y. [2012] "Plan for Next Generation Attenuation for subduction earthquakes," *Proceedings U.S. Geological Survey Workshop 2014 National Seismic Hazard Maps*, Seattle, WA.
- Campbell K.W., Bozorgnia Y. [2007] "Campbell-Bozorgnia NGA ground motion relations for the geometric mean horizontal component of peak and spectral ground motion parameters," *PEER Report 2007/02*, Pacific Earthquake Engineering Research Center, Berkeley, CA.
- Collins N., Graves R.W., Somerville, P.G. [2006] "Comparison of validations of ground motion simulation procedures," *Report to the PEER-Lifelines Program, Project 1C02d*. URS Corporation, Pasadena Office, 26 pgs.
- Hikita T. [2006] "Characteristics of strong ground motions at the forward rupture direction," *12th Japan Earthquake Engineering Symposium*, 4 pgs.
- Howard J K., Tracy C A., Burns R.G. [2005] "Comparing observed and predicted directivity in near-source ground motion," *Earthquake Spectra*, Vol. 21, No. 4, pp. 1063–1092.
- Huang Y.-N., Whittaker A.S., Luco N. [2008] "Maximum spectral demands in the near-fault regions," *Earthquake Spectra*, Vol. 24, No. 1, pp. 319–341.
- Huang Y.-N., Whittaker A.S., Luco N. [2012] "Maximum spectral demand in the United States," U.S. Geological Survey, *USGS Open-File Report*, in preparation, 217 pgs.

- Kato K., Masayuki T., Kazuhiko Y. [2002] "Rupture directivity effect in near fault regions-numerical studies for the great inter-plate earthquakes," *Proceedings of the Japan Earthquake Engineering Symposium*, Vol. 11, pp. 145–150.
- Mai P.M, Spudich P., Boatwright J [2005] "Hypocenter locations in finite-source rupture models," *Bulletin of the Seismological Society of America*, Vol. 95, No. 3, pp. 965–980.
- NEHRP [2009] *NEHRP Recommended Seismic Provisions for New Buildings and Other Structures*, 406 pgs.
- NIST [2011] "Selecting and scaling earthquake ground motions for performing response-history analyses," National Institute of Standards and Technology, *Report number GCR 11-917-15*, prepared by the NEHRP Consultants Joint Venture, Gaithersburg, MD, 256 pgs.
- Rowshandel B. [2006] "Incorporating source rupture characteristics into ground-motion hazard analysis models," *Seismological Research Letters*, Vol. 77, No. 6, pp. 708–722.
- Rowshandel B. [2010] "Directivity correction for the Next Generation Attenuation (NGA) relations," *Earthquake Spectra*, Vol. 26, No. 2, pp. 525–559.
- Sesetyan K. [2007] *Characterization of Response Spectra For Near Field Conditions by Earthquake Ground Motion Simulation*, PhD. Thesis, Bogazici University, Istanbul.
- Shahi S.K., Baker J.W. [2011] "An empirically calibrated framework for including the effects of near-fault directivity in probabilistic seismic hazard analysis," *Bulletin of the Seismological Society of America*, Vol. 101, No. 2, pp. 742–755.
- Shahi S.K., Baker J.W. [2012] "Preliminary NGA-West 2 models for ground-motion directionality," *Proceedings 15th World Conference on Earthquake Engineering*, Lisbon, Portugal.
- Si H., Midorikawa S. [2004] "Evaluation of rupture directivity effects on strong ground motion based on hybrid simulation method," *Proceedings 13th World Conference on Earthquake Engineering*. Vancouver, B.C., Canada.
- Somerville P.G. [2002] "Characterizing near fault ground motion for the design and evaluation of bridges," *Proceedings 3rd National Seismic Conference & Workshop on Bridges & Highways*, Portland, OR.
- Somerville P.G. [2003] "Magnitude scaling of the near fault rupture directivity pulse," *Physics of the Earth and Planetary Interiors*, Vol. 137, No. 1, pp. 201–212.
- Somerville P.G., Smith N.F., Graves R.W., Abrahamson N.A. [1997] "Modification of empirical strong ground motion attenuation relations to include the amplitude and duration effects of rupture directivity," *Seismological Research Letters*, Vol. 68, No. 1, pp. 199–222.
- Spudich P., Chiou, B.S.J. [2008] "Directivity in NGA earthquake ground motions: Analysis using isochrone theory," *Earthquake Spectra*, Vol. 24, No. 1, pp. 279–298.
- Spudich P., Chiou B.S.J., Graves R.W., Collins N., Somerville P.G. [2004] "A formulation of directivity for earthquake sources using isochrone theory," U.S. Geological Survey, *USGS Open-File Report 2004-1268*, Menlo Park, CA.
- Spudich P., Somerville P.G., Shahi S.K., Rowshandel B., Chiou B.S.J., Bayless J., Baker J.W. [2012] "Directivity models produced for the Next Generation Attenuation West 2 (NGAW2) project," *Proceedings of 15th World Conference on Earthquake Engineering*, Lisbon, Portugal.
- Watson-Lamprey J., Boore D.M. [2007] "Beyond SaGMRotI: Conversion to SaArb, SaSN, and SaMaxRot," *Bulletin of the Seismological Society of America*, Vol. 97. No. 5, pp. 1511–1524.